Proceedings of the SPIE Optical Diagnostics for Fluids, Solids, and Combustion II. 3-4 August 2003,
San Diego, CA, USA. Volume 5191, 113. Eds. Patrick V. Farrell, Fu-Pen Chiang, Carolyn R. Mercer, Gongxin Shen

Dual Illumination Planar Doppler Velocimetry using a Single Camera

Tom O. H. Charrett, Helen D. Ford, David S. Nobes and Ralph P. Tatam*
Optical Sensors Group, Centre for Photonics and Optical Engineering, School of Engineering,
Cranfield University, Cranfield, Bedford, MK43 0AL, UK.

ABSTRACT

A Planar Doppler Velocimetry (PDV) illumination system has been designed which is able to generate two beams, separated in frequency by about 600 MHz. This allows a common-path imaging head to be constructed, using a single imaging camera instead of the usual camera pair. Both illumination beams can be derived from a single laser, using acousto-optic modulators to effect the frequency shifts.

One illumination frequency lies on an absorption line of gaseous iodine, and the other just off the absorption line. The beams sequentially illuminate a plane within a seeded flow and Doppler-shifted scattered light passes through an iodine vapour cell onto the camera. The beam that lies at an optical frequency away from the absorption line is not affected by passage through the cell, and provides a reference image. The other beam, the frequency of which coincides with an absorption line, encodes the velocity information as a variation in transmission dependent upon the Doppler shift. Images of the flow under both illumination frequencies are formed on the same camera, ensuring registration of the reference and signal images. This removes a major problem of a two-camera imaging head, and cost efficiency is also improved by the simplification of the system.

The dual illumination technique has been shown to operate successfully with a spinning disc as a test object. The benefits of combining the dual illumination system with a three-component, fibre-linked imaging head developed at Cranfield will be discussed.

Keywords: Planar Doppler Velocimetry, flow measurement, acousto-optic frequency switching

1. INTRODUCTION

Planar Doppler velocimetry (PDV)[1,2,3,4] is a flow measurement technique that provides velocity information over a plane defined by a light sheet formed from an expanded laser beam. The optical frequency of light scattered from each particle in the seeded flow experiences a Doppler shift, which is linearly related to the velocity of the particle at that point in the flow. In PDV, a region of the illuminated flow is imaged, through a glass cell containing iodine vapour, onto the active area of a CCD camera. Iodine has numerous narrow absorption lines over a large part of the visible spectrum[5,6]. There are sufficient lines that one or more fall within the gain curves of several commonly used laser sources. If the laser frequency is chosen to coincide with one such line, the optical intensity at any position in the camera image is a function of the Doppler shift experienced at the corresponding flow position, via the frequency-dependent iodine absorption.

The intensity over a PDV image is affected by the intensity profile of the illuminating laser sheet (typically Gaussian), spatial variations of the seeding density within the flow, and diffraction fringes caused by imperfections in the optical surfaces. These variations are generally of similar amplitude to those resulting from absorption in the iodine cell, and can obscure the information about flow velocity that is contained within the camera image. It is therefore usual to amplitude-divide the image beam onto two cameras; from one of the two imaging paths the iodine cell is omitted, and the resulting image acts as a reference to normalise the signal image carrying the velocity information.

Superposition of the reference and signal images to sub-pixel accuracy is essential if errors in the calculated velocities are to be avoided. Errors due to poor image registration can become particularly troublesome if large velocity gradients are present in the region imaged. The main causes of poor image registration are differences between the optical aberrations and magnifications of the two imaging paths. Thus errors tend to be worse towards the outside edges of the images, where these factors are largest. Software de-warping routines can improve pixel matching[7] and can help to

* r.p.tatam@cranfield.ac.uk; phone +44 (0) 1234 754630; fax +44 (0) 1234 751566; http://www.cranfield.ac.uk/sme/cpoe/osg.htm

correct for small differences in magnification. Post-processing cannot, however, correct for the almost inevitable differences in the optical distortions.

This paper describes a technique for generating dual illumination beams at 514.5 nm, differing in optical frequency by 600 MHz. By toggling between the two beams, reference and signal images can be acquired on a single CCD camera.
An absorption line of iodine lies under the gain curve of an argon-ion laser, close to the centre of the curve. The 514.5 nm line of the laser is tuned just off the low frequency side of the absorption line and the beam is divided into two, travelling through an optical arrangement containing a pair of acousto-optic modulators (AOMs) chosen to generate a total frequency shift of 600 MHz. The first AOM provides an 80 MHz shift, and is used to upshift the frequency of one beam. The other device provides a 260 MHz shift, and is used in a double pass configuration so that there is an overall 520 MHz downshift on the second beam. Thus the resultant frequency difference between the two illumination beams is 600 MHz. This is sufficient to take the optical frequency from a position off the side of the iodine absorption line to a position close to the 50% absorption level on this side of the line. Since the original laser frequency is off the absorption line, this beam will pass unaffected through the iodine cell. Thus, illumination beams appropriate for acquisition of both reference and signal images can be derived from the same source, and a common path optical geometry becomes possible, where the PDV system is reduced simply to an iodine cell positioned directly in front of the lens of the solid-state camera. Furthermore, since the wavelength difference between the two beams is negligible in comparison with the typical size of scattering particles, the scattering efficiency should be identical for the two beams at any particular orientation. Exact alignment of the reference and signal images on the active area of the camera is automatic. The method also eliminates the polarisation differences between the two beam paths that occur in the two-camera system, and which are not completely eliminated even by the use of a polarisation-independent beam splitter.
The system outlined here represents an advance on a previous configuration we have investigated[8], in which only the 260 MHz AOM was used for frequency-shifting. The original arrangement did not allow for total separation of the signal and reference images; acquired images were illuminated either by the reference beam alone, or by the reference and signal beams together. This meant that an additional subtraction step was required in processing the two frames, to extract the signal information alone. Signal-to-noise is expected to improve in the new configuration, as the reference and signal images are acquired completely independently.

The disadvantage of the system described above is that acquisition can no longer be perfectly simultaneous for the reference and signal images. Since the images are not spatially separated, they must instead be separated in time. For steady-state flows this is not a major difficulty, provided that the seeding is relatively dense and the seeding distribution remains essentially unchanged during the time taken to acquire the two image frames. The extent to which this condition is satisfied will depend upon the flow situation. The accuracy of measurements made in a steady-state flow can be improved by acquiring a succession of image pairs and averaging the normalised intensity maps over an extended period.

2. METHOD

2.1 Illumination system

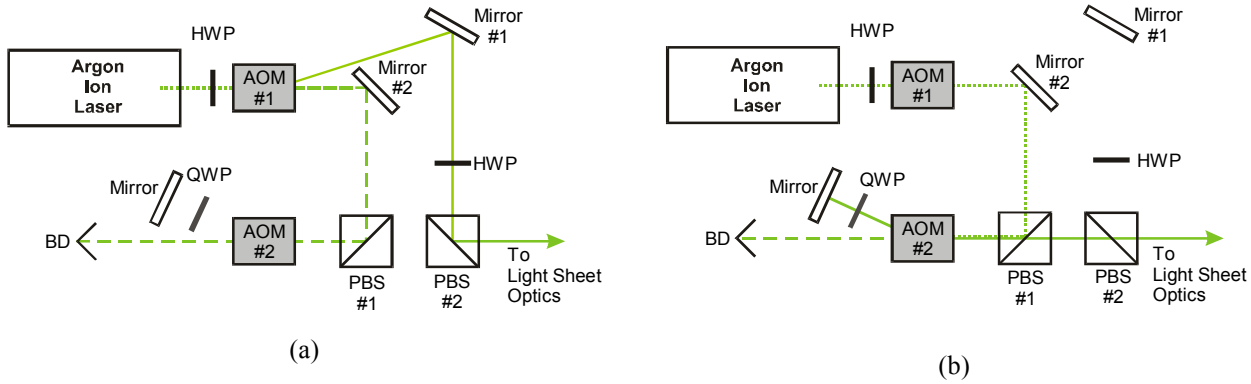

Figure 1. Schematic of the CW dual illumination PDV system. (a) The reference beam. (b) The signal beam. HWP - λ/2 plate; AOM – acousto-optic modulator; PBS – polarising beam splitter, QWP – λ/4 plate; BD – beam dump.
Laser Beam Shifted Laser Beam. Unshifted Laser beam

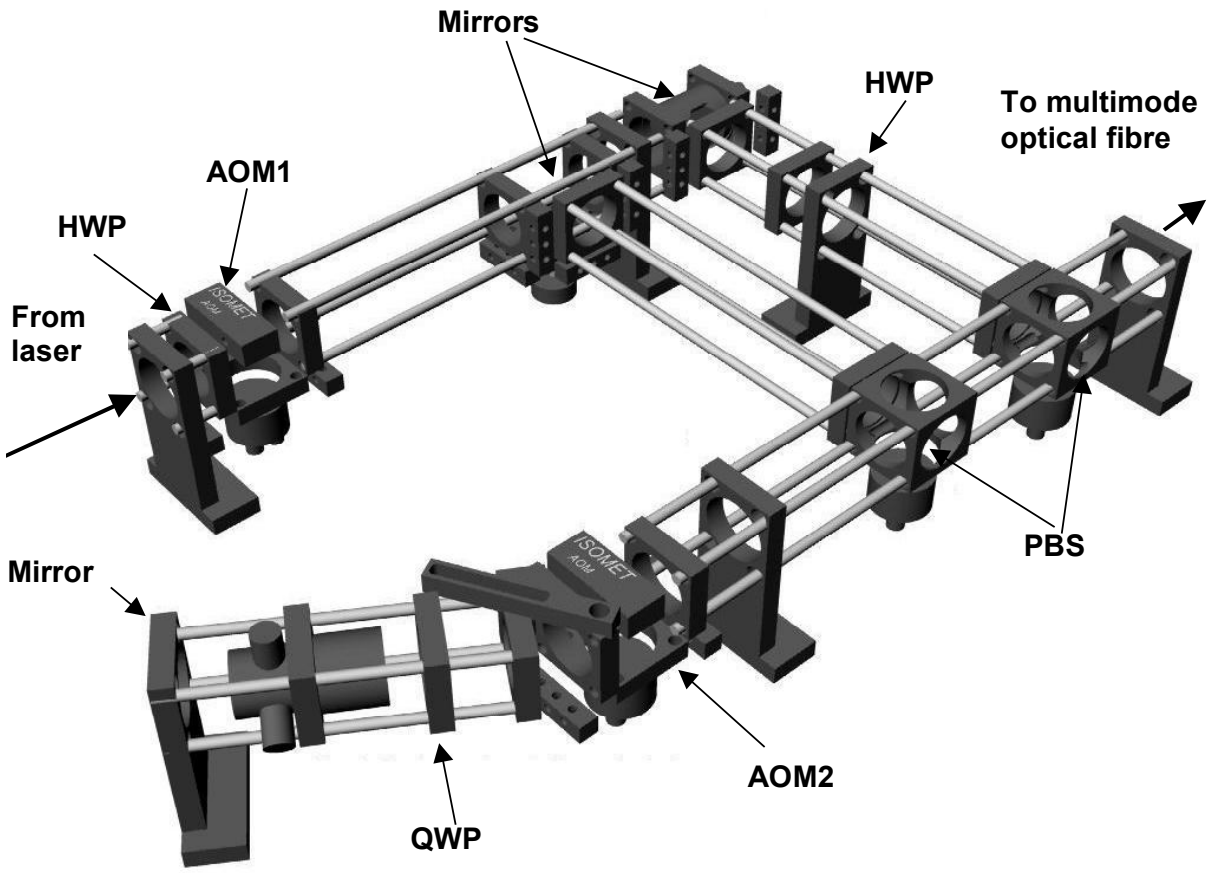

Figure 2: 3-D representaion of the dual illumination configuration; HWP – half-wave plate, QWP – quarter-wave plate, AOM – acousto-optic modulator, PBS – polarising beam splitter.

A pair of diagrams showing the configuration and operation of the dual illumination system is shown in figure 1, and a 3-dimensional representation of the system constructed in Linos 'microbench' is presented in figure 2. The original laser beam passes first through a half-wave plate (HWP) to adjust the polarisation azimuth and then through an acousto-optic modulator (AOM1). When AOM1 is switched on, the first order beam experiences a frequency shift of 80 MHz and is deflected through the Bragg angle. There is some loss of power as the process is not 100% efficient. Beam steering optics then redirect this beam into a position from which it can be coupled into a multimode optical fibre. The second half-wave plate, orientated so as to rotate the polarisation azimuth through 90^{o}, is necessary to achieve reflection of the beam at the polarising beam splitter cube.

Conversely, when AOM1 is switched off, the beam passes through with no frequency shift or angular deflection, and is incident upon a second mirror, which directs it into an alternative beam path. This beam passes through a telescope, reducing the diameter of the beam by a factor of about three. The reduced beam diameter is sufficiently small to allow the beam to pass through the active area of AOM2 positioned in the system, by which the optical frequency is altered by 260 MHz. The shifted beam is then retroreflected by a mirror, making a double pass through a quarter wave plate (QWP), which rotates the polarisation state by 90^{o}. The beam makes a second transit through the AOM, doubling the optical frequency shift to a total of 520 MHz , and is recombined with the reference beam in the output PBS and coupled into the optical fibre.

In our previous work, the two beams were transported to the measurement region by a single-mode polarisation-preserving optical fibre[9]. The light that emerges from the optical fibre is a clean, spatially filtered beam with an approximately Gaussian intensity profile. However, when the Gaussian beam is formed into a light sheet, this also has a Gaussian intensity profile, implying reduced intensity away from the centre axis of the sheet. In the modified system, beams are coupled into a multimode fibre, and are no longer formed into a sheet. Instead, a prism scanning device is used to scan the collimated beam rapidly across the region of interest, resulting in an ideal 'top-hat' intensity profile and avoiding the diffraction artefacts previously caused by imperfections in the sheet-forming optics[10].

The light source was a tuneable Argon-ion laser (Spectra Physics Beamlok 2060), incorporating a temperature-stabilised etalon to ensure single-mode operation at 514.5 nm. The single-mode linewidth was about 2 MHz which, as may be seen in section 2.2 below, is about three orders of magnitude lower than the width of the absorption line and can therefore be neglected in considering the absorption-related intensity variation. Wavelength stability was about 3 MHz, plus a long term drift with ambient temperature of about 40 MHz K^{-1}. Both signal and reference beams experience scattering from the flow, and the frequency shifts imposed on each beam are identical. Since both beams also pass through the iodine cell, the initial reference frequency must be positioned sufficiently far from the top of the absorption line that the maximum Doppler shift expected in the system will not bring it down below the top of the line.

2.2 Image-capture system

As described in the introduction, the image-capture system is greatly simplified compared with that required for a standard system using a single illumination frequency. Both reference and signal beams pass through the iodine cell and, for measurement of a single velocity component, the system is reduced to a single solid state CCD camera incorporating a zoom lens, together with a temperature-stabilised iodine cell positioned directly in front of the lens.

The camera used for image capture is an 'Imager Intense' supplied by LaVision. It is a digital camera with 12 bit A/D conversion on a Peltier-cooled chip, and approximately 1K by 1K image resolution. Dedicated image acquisition and processing software (called DaVis) is used to control the camera and to calculate and display normalised intensity maps. The integration time of the camera can be varied between 1 ms and 1000 s, depending on the scattered light intensity. The iodine cell, which operates as a saturated cell[11], is 25 mm in diameter and 50 mm long, with a cold finger. The cold finger is held at 40^{o} C using a Peltier element in a feedback loop, and the cell body is contained in an oven held at 56.5^{o} C.

Accurate velocity measurements using PDV require an exact knowledge of the shape of the iodine absorption line as a function of frequency. This is obtained by monitoring the intensity of a low-power, unexpanded beam after passage through the iodine cell, as the laser frequency is scanned at a constant rate across the frequency range around the absorption line. The Spectra-Physics argon-ion laser used in the project allows the laser frequency to be scanned by applying a voltage ramp to a modulation input that controls etalon temperature. Because the modulation is temperature based, it must be carried out rather slowly to avoid instability and mode hopping. A reset occurs after a scan range approaching 1 GHz. Since the FWHM of the absorption line is also about 1 GHz, an uninterrupted plot of the relevant section of the iodine line can generally be obtained. Otherwise two scans may be concatenated to cover the desired range. A plot of iodine transmission as a function of optical frequency is shown in figure 3, together with a sixth-order polynomial fit. This is approximately Gaussian in form, and the near-linear region between the normalised absorption values of 0.2 and 0.8 corresponds to a frequency range of about 300 MHz. For practical illumination/viewing geometries, this typically allows measurement of flow velocities from a few metres per second up to a few hundred metres per second. Measurement error, as a fraction of the measured value, is lower for higher flow velocities.

Synchronisation of image capture with the appropriate illumination beams was achieved by applying a voltage to the AOM drivers prior to each operation of the electronic shutter. The 260 MHz AOM is TTL addressable and could, in principle be switched on and off up to MHz frequencies, but the 80 MHz AOM does not have this facility. Pairs of images were collected and stored for processing.

In its simplest form, processing the images consists of background subtraction, then division of the signal image by the reference image. De-warping is not essential, since image registration is automatic, though severe aberration may distort the image of the planar light sheet onto a curved surface at the camera. This was not the case in our optical system, which was carefully designed to minimise aberrations. Typically, the reference and signal illumination beams will be of

different power, so a normalisation factor must be included to account for this in taking the ratio between the images. It is important also to take background images for each illumination beam independently, because of the difference in delivered power and therefore in background scattered light.

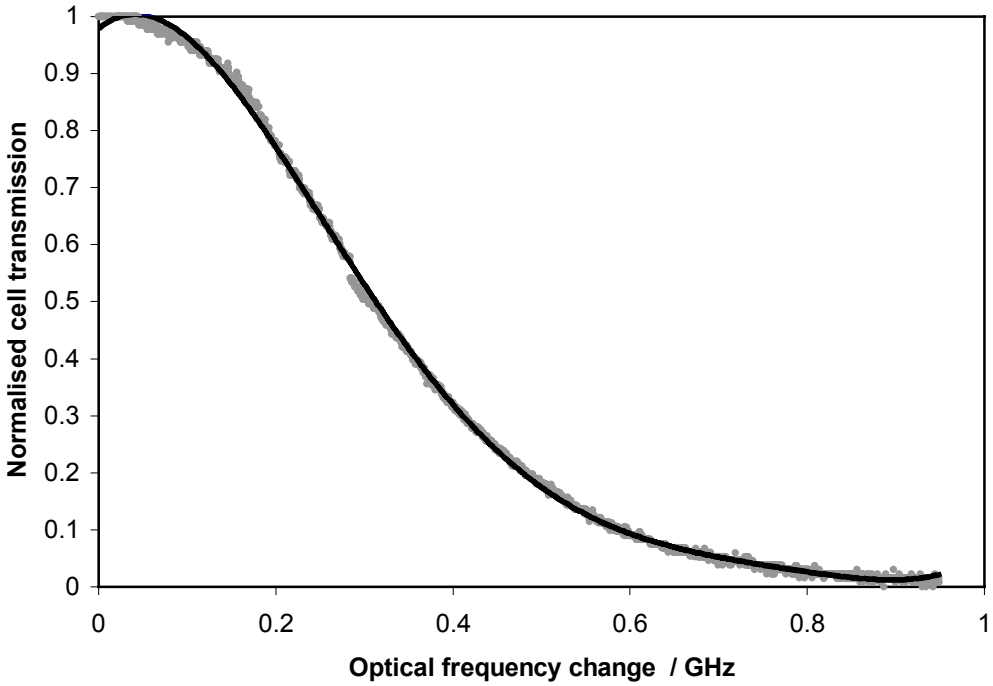

Figure 3: Plot showing the normalised transmission of the iodine vapour cell as a function of laser frequency (circles), and a sixth-order polynomial fit to the data (solid line).

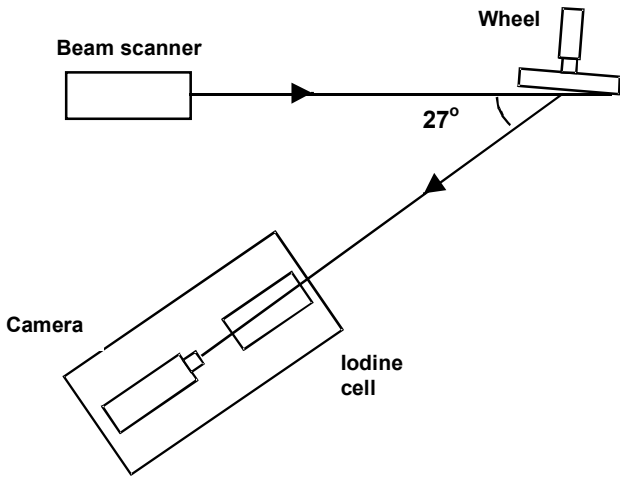

Figure 4: Experimental illumination and observation arrangement.

The test object used to assess the PDV system was a perspex wheel 200 mm in diameter, coated with matt white paint and mounted centrally on the spindle of a rotary motor such that the plane of the disc was orthogonal to the plane of the optical bench. The maximum rotation rate of the wheel was about 54 Hz, corresponding to a circumferential velocity of 34 ms^{-1}. Figure 4 shows a plan view of the experimental arrangement. The backscatter geometry is chosen to have high sensitivity to the horizontal component of rotational velocity in the plane of the wheel.

The expected frequency shift is given by the usual Doppler equation

$$\Delta\nu = \frac{\nu(\bar{\mathbf{o}} - \bar{\mathbf{i}}).\mathbf{v}}{c},$$

where ν is the optical frequency, $\bar{\mathbf{o}}$ and $\bar{\mathbf{i}}$ are unit vectors in the observation and illumination directions respectively, $\mathbf{v}$ is the velocity vector and c is the speed of light in air. The horizontal component of velocity is expected to vary linearly along any vertical line through the disc.

3. RESULTS

Sets of image pairs were stored for both anticlockwise and clockwise rotation of the disc, as viewed from the front, at the maximum rotation speed. The optical power at the output of the optical fibre was about 2 mW, and the integration time on the cameras was about 40 s. AOMs were toggled on or off to provide the appropriate illumination for each image. The illumination intensity profile actually varied slightly for reference and signal illumination beams, possibly due to differences in the mode mixing within the multimode fibre. The fibre did not transmit a large number of modes, and the output mode pattern in this case is very sensitive to the optical coupling geometry at the fibre input. Because of the differing intensity profiles, a 'white card' image was taken for each illumination beam, with the laser tuned off the absorption line. This was used to normalise the individual signal and reference images.

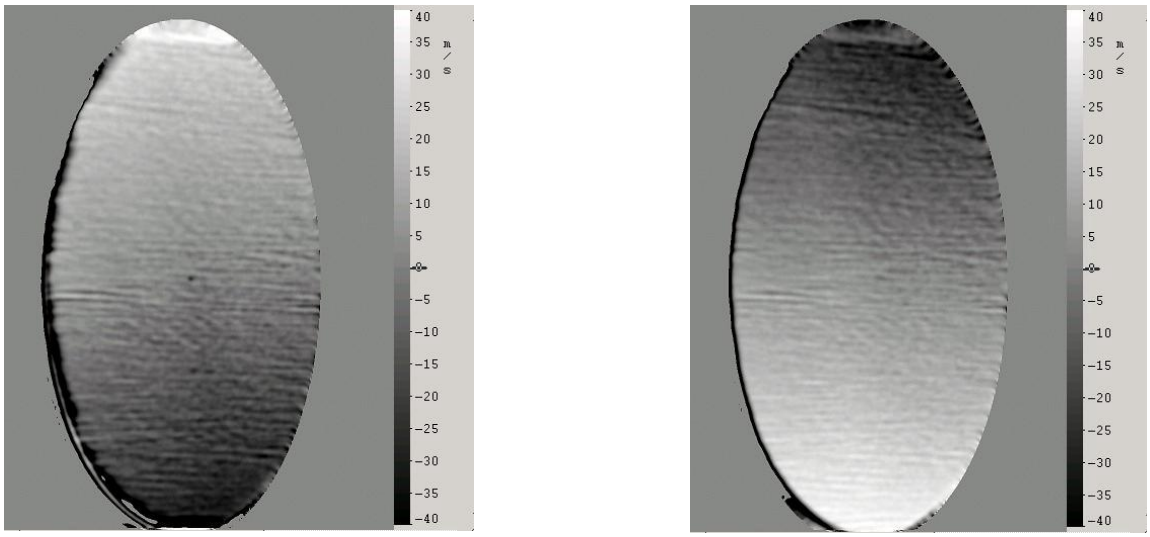

(a) (b)

Figure 5: Normalised and smoothed intensity maps, incorporating the 'white card' correction for variation in illumination beam profiles for (a) anticlockwise and (b) clockwise rotation of the disc.

The image analysis, which is carried out using the DaVis software by loading the stored images into memory buffers, simply comprises division of each raw image by the corresponding 'white card' image, and then taking a ratio of the resulting signal and reference images. 12-bit digitisation is used for image storage and manipulation. The normalised image can be displayed using either a greyscale or a false colour format. For the images shown in figure 5, the signal illumination frequency was positioned well down the side of the iodine absorption line, in the approximately linear region. Therefore the greyscale value for each pixel, which represents the Doppler shift for that position on the wheel, should be linearly related to the wheel velocity at the same position. The greyscale value at the centre of the disc in each image corresponds to a Doppler shift of zero, since this position on the wheel has zero velocity. If the laser frequency remains stable, this value should be constant for all stored images.

The normalised images obtained immediately after performing the ratio operation are quite noisy, and those displayed above have undergone smoothing with a 7x7 averaging filter. The result of this process will be to improve the signal-to-noise ratio of the measure velocity, but to decrease the spatial resolution. The spatial resolution of the unsmoothed data, at the magnification used in this experiment, is approximately 400 μm, and some loss of resolution can be tolerated while still retaining a sufficient density of data across the image area. The spatial resolution required will depend on the flow being investigated. Pixel binning can be used as an alternative to an averaging filter, and has a similar effect.

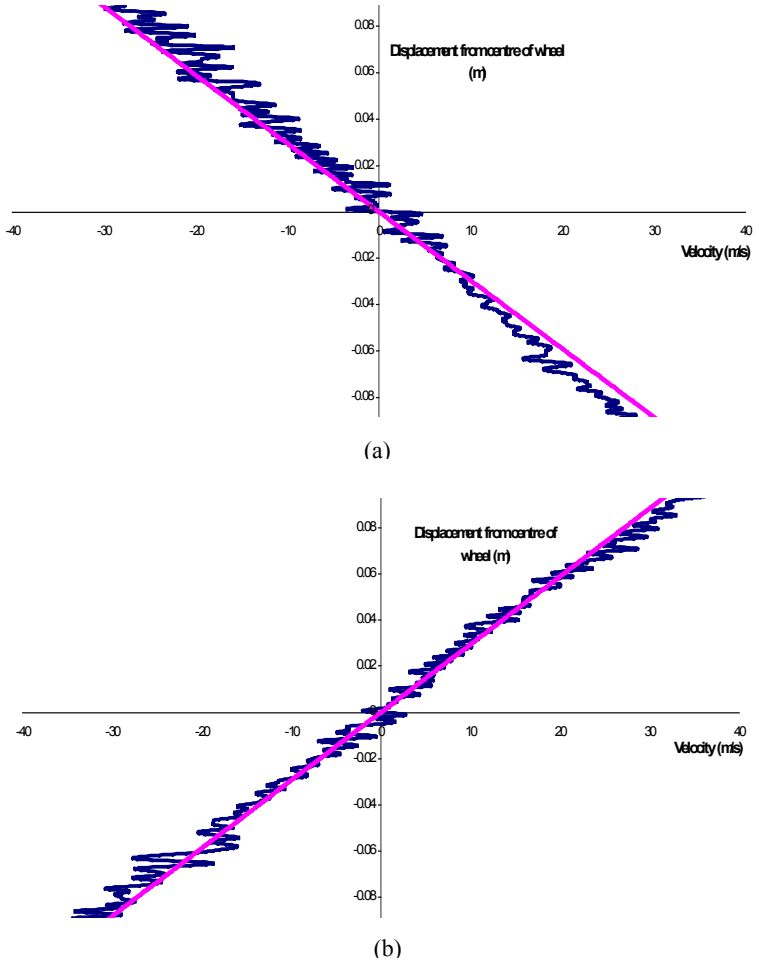

Figure 6: Intensity profiles taken from the images of figure 6 on a vertical column passing through the centre of the disc for (a) anticlockwise and (b) clockwise rotation. In each case a linear fit is superimposed over the image data.

Profiles of the greyscale value were taken vertically through the smoothed images of figure 5, passing through the centre of the disc. Figure 6 (a) shows a profile taken through the averaged image for anticlockwise rotation, and 6 (b) the profile for clockwise rotation of the wheel. As expected, the velocity gradient is negative for the first plot, and positive for the second, corresponding to the reversal in the sense of rotation. Each plot shows a linear fit superimposed on the data. The velocity error for these plots is about +/- 2 ms^{-1}. The advantage of the beam scanning system over a light sheet generated using cylindrical optics is that the intensity is reasonably constant across the whole image area, and therefore the signal-to-noise ratio (SNR) also remains fairly constant across the whole profile. Previously, using a light sheet, the SNR was much worse towards the edges of the image, where light levels were lower.

4. DISCUSSION

The results presented above follow on from previous work carried out in our laboratory, in which the use of a single AOM indicated that frequency-switching can provide accurate PDV velocity data from a spinning disc. Processing is made extremely straightforward in the one camera system, by the avoidance of any pixel-matching requirement. In the previous configuration, the reference and signal beam illumination appeared together on one image, with the reference beam alone on the other image. The image calculations therefore involved an additional subtraction step, which is no longer required in the configuration shown here, since the use of two AOMs allows the reference and signal beam illumination to be separated completely into two independent images.

The use of the beam scanner instead of cylindrical sheet-forming optics also improves the quality of the images obtained, since the distribution of intensity across the entire image region is now much more even. Work is continuing on the illumination system, to investigate the reason why the illumination profiles still differ slightly for the reference and signal beams. It should be possible to adjust the lens and mirror arrangement in the scanner to obtain identical beam profiles for both inputs, approximating the ideal 'top-hat' beam profile. This would remove the necessity for the 'white card' normalisation step in the processing, which would not be straightforward to perform in a real flow, and inevitably lowers the SNR in the calculated velocities.

The power available at the output of the multimode fibre is currently about 2-6 mW from a laser output of about 600 mW which, although very inefficient, is sufficient for making measurements on the rotating wheel at integration times of a few tens of seconds. A significant amount of power is lost because the optical arrangement includes many surfaces, few of which are anti-reflection coated at 514 nm. Efficiency would be improved by substituting coated optics. The major losses, however occur in the AOMs. The 260 MHz AOM has a very small aperture and a first-order efficiency of less than 50%, and two passes are made through this component. Up to ten times more power is available in the other beam path, since the 80 MHz AOM has a much larger aperture and is more efficient. Components are now available with improved efficiencies and offering larger wavelength shifts, so we expect to be able to improve the available power from the system to a level more usable in real flows. For example, using two 350 MHz AOMs in single pass, at least an order of magnitude improvement in delivered power would be expected; possibly up to two orders of magnitude, which would result in 100-200 mW in the measurement volume. It should also be remembered that we are currently scanning across a relatively large area (200 mm displacement) which may be unnecessarily large in some situations.

For the camera exposure times used in these experiments, the optical power in the scattered beam remains constant with time, as it is always integrated over many complete rotations of the wheel. An important difference in a real flow is that the scattered power, and its distribution over the camera image, may change between acquisition of the reference and signal images. In a steady-state flow, if the seeding remains fairly uniform, the errors caused by this should remain small, and can be minimised by taking an average over many normalised images. The number of images required for acceptable performance will depend on the nature of the flow. Future plans include testing the system on a ducted airflow, using seeding from a smoke generator.

In a rapidly time-varying flow, of course, averaging over many images is not an option, and application of the technique is not straightforward. A pulsed laser would be required for this type of flow[12], to freeze the motion of the particles. With state-of-the-art cameras, the time between two frames can be as short as 100 ns, so near-simultaneous acquisition would be possible. This would be acceptable for many moderate-speed flows.

An innovative three-component PDV system has been developed at Cranfield under a separate programme[13,14], using a coherent optical fibre bundle to transmit three views of the flow, monitored from different viewpoints, back to the camera. The small size of the bundle means that it is still possible to operate with a single camera and cell, while now

obtaining full 3D flow information. The bundle-based viewing system, which is described in detail in paper 5191-23 of this conference, can be used with the dual illumination configuration to obtain 3D data, provided that sufficient optical power is available.

5. CONCLUSIONS

It has been shown that a PDV illumination system using dual-frequency illumination generated by two acousto-optic modulators, and fibre-delivered to the measurement region, can eliminate one of the cameras from the conventional Planar Doppler Velocimetry (PDV) sensing head. Automatic superposition of the signal and reference images is achieved, and polarisation errors caused by the beam splitter in the conventional system are eliminated. The system presented is an improvement on a previous configuration that included only a single AOM. The modified version permits complete separation of the signal and reference data and simplifies the processing required. The system has been tested on a rotating wheel, and is currently achieving a velocity resolution of about +/-2 ms^{-1}.

ACKNOWLEDGMENTS

This work was partially supported by the Engineering and Physical Sciences Research Council (EPSRC) UK, under grant GR/504291, and by the Royal Society UK.

REFERENCES

1. H. Komine, S. Brosnan, A. Litton and E. Staepperts, "Real-Time Doppler Global Velocimetry", *AIAA Paper 91-0337*, 1991.
2. J.F. Meyers, "Development of Doppler Global Velocimetry as a Flow Diagnostic Tool", *Measurement Science and Technology*, **6**, pp 769-783, 1995.
3. E. Irani and L.S. Miller, "Evaluation of a Basic Doppler Global Velocimetry System", *Society of Automotive Engineers, Paper 951427*, 1995.
4. H.D. Ford and R.P. Tatam, "Development of Extended Field Doppler Velocimetry for Turbomachinery Applications", *Optics and Lasers in Engineering*, **27**, pp 675-696, 1997.
5. S. Gerstenkorn and P. Luc, "Atlas du Spectre d'Absorption de la Molecule d'Iode 14800-2000 cm^{-1} Complement: Identification des Transitions du Systeme (B-X)", Laboratoire Aime-Cotton, Centre Nationale de la Recherche Scientifique, Orsay, France, 1986.
6. V.S.S. Chan, A.L. Heyes, D.I. Robinson and J.T. Turner, "Iodine Absorption Filters for Doppler Global Velocimetry", *Measurement Science and Technology*, **6**, pp 784-794, 1995.
7. R.J. Manners, S.J. Thorpe and R.W. Ainsworth, "Image Processing Techniques for Doppler Global Velocimetry", *Proc. I. Mech. E. Conference on Optical Methods and Data Processing in Heat and Fluid Flow*, London, 1996.
8. H.D.Ford, D.S. Nobes and R.P. Tatam, "Acousto-Optic Frequency Shifting for Single-Camera Planar Doppler Velocimetry", *SPIE Proceedings, Optical Diagnostics for Fluids, Solids and Combustion*, Eds. C.R. Mercer, S.S. Cha and G. Shen, Vol. 4448, pp 272-282, San Diego, 2001.
9. S.C. Rashleigh, "Origins and Control of Polarization Effects in Single-Mode Fibers", *Journal of Lightwave Technology*, **LT-1**, 312-331, 1983.
10. I. Roehle, R. Shodl, P. Voigt and C. Willert, "Recent Developments and Applications of Quantitative Laser Light Sheet Measuring Techniques in Turbomachinery Components", *Measurement Science and Technology*, **11**, pp 1023-1035, 2000.
11. T.J. Quinn and J.-M. Chartier, "A New Type of Iodine Cell for Stabilized Lasers", *IEEE Transactions on Instrumentation and Measurement*, **42**, 405-406, 1993.
12. R.L. McKenzie, "Measurement Capabilities of Planar Doppler Velocimetry Using Pulsed Lasers", *AIAA Paper 95-0297*, 1995.
13. D.S. Nobes, H.D. Ford and R.P. Tatam, "Instantaneous, Two-Camera, Three-Dimensional Planar Doppler Velocimetry Using Imaging Fibre Bundles", *SPIE Proceedings, Optical Diagnostics for Fluids, Solids and Combustion*, Eds. C.R. Mercer, S.S. Cha and G. Shen, Vol. 4448, pp 72-83, San Diego, 2001.
14. D.S. Nobes, H.D. Ford and R.P. Tatam, "Three Component Planar Doppler Velocimetry Using Imaging Fibre Bundles", *Experiments in Fluids*, (in press).